Wavelength-tunable (1.55- μm region) InAs quantum dots in InGaAsP/InP (100) grown by metal-organic vapor-phase epitaxy

Wavelength-tunable (1.55-μm region) InAs quantum dots in InGaAsP/InP (100) grown by metal-organic vapor-phase epitaxy

S. Anantathanasarn,[a] R. Nötzel, P. J. van Veldhoven, T. J. Eijkemans, and J. H. Wolter
European Institute for Telecommunication Technologies (eiTT)/Inter-University Research Institute on Communication Technology: Basic Research and Applications (COBRA), Eindhoven University of Technology, 5600 MB Eindhoven, The Netherlands

(Received 2 March 2005; accepted 28 April 2005; published online 1 July 2005)

Growth of wavelength-tunable InAs quantum dots (QDs) embedded in a lattice-matched InGaAsP matrix on InP (100) substrates by metal-organic vapor-phase epitaxy is demonstrated. As/P exchange plays an important role in determining QD size and emission wavelength. The As/P exchange reaction is suppressed by decreasing the QD growth temperature and the V/III flow ratio, reducing the QD size and emission wavelength. The As/P exchange reaction and QD emission wavelength are then reproducibly controlled by the thickness of an ultrathin [zero to two monolayers (MLs)] GaAs interlayer underneath the QDs. An extended interruption after GaAs interlayer growth is essential to obtain well-defined InAs QDs. Submonolayer GaAs coverages result in a shape transition from QD to quantum dash at low V/III flow ratio with a slightly shorter emission wavelength. Only the combination of reduced growth temperature and V/III flow ratio with the insertion of GaAs interlayers above ML thicknesses allows wavelength tuning of QDs at room temperature in the technologically important 1.55-μm wavelength region for fiber-optical telecommunication systems. A GaAs interlayer thickness just above one ML produces the highest photoluminescence (PL) efficiency. Temperature-dependent PL measurements reveal zero-dimensional carrier confinement and defect-free InAs QDs. © *2005 American Institute of Physics*. [DOI: 10.1063/1.1938271]

I. INTRODUCTION

Quantum dot (QD) active regions in optical devices such as lasers and semiconductor optical amplifiers (SOAs) have great potential based on the singular energy dependence of the density of states of QDs. This provides drastic improvements of device performance in terms of high gain, low-threshold current, and high characteristic temperature.[1,2] With regard to the fabrication methods, the direct epitaxial growth of self-assembled QDs in the Stranski–Krastanov (SK) mode in lattice-mismatched materials systems has proven to realize high-quality coherent and virtually defect-free QDs. Therefore, aiming at devices operating in the 1.55-μm wavelength region, self-assembled InAs QDs embedded in an InGaAsP matrix lattice-matched to InP (100) substrates are an attractive choice for applications in fiber-optical telecommunication systems.

Controlling, however, the emission wavelength of InAs/InP QDs in the 1.55-μm region is still a challenge. This is primarily due to the small lattice mismatch (3.2%), resulting in relatively large QDs and the presence of As/P exchange during InAs growth on the InGaAsP surface,[3,4] inevitably contributing to the QD growth, shifting the emission wavelength beyond 1.6 μm at room temperature (RT).[5] In fact, large InAs islands have even been observed on InP surfaces after a few seconds of annealing under AsH_3 flow.[6] Attempts to control the QD emission wavelength by thin capping and annealing usually resulted in enhanced size fluctuations producing multiple peaks in photoluminescence (PL) measurements.[7] PL emission and lasing at 1.55 μm were achieved with quasi-one-dimensional InAs/InP quantum dashes instead of zero-dimensional QDs grown by molecular-beam epitaxy (MBE), which, however, behave more like quantum wires with relatively weak lateral carrier confinement.[8]

We have recently proposed and demonstrated a method to reproducibly tune the emission wavelength of InAs/InP QDs grown by chemical-beam epitaxy (CBE) in the 1.55-μm wavelength region by the insertion of ultrathin [zero to two monolayers (MLs)] GaAs interlayers between the QDs and the InGaAsP layer underneath. As a function of thickness, the GaAs interlayer effectively suppresses the As/P exchange reaction, which continuously reduces the QD height to tune the emission wavelength from above 1.6 μm to below 1.55 μm at RT.[9] This is related to the binary- compound bond strengths. The In–As bond (bond enthalpy of 48.0 kcal/mol) is more stable than the In–P bond (47.3 kcal/mol), favoring the replacement of P bound to In by As. On the contrary, both the Ga–P and Ga–As bonds are more stable than the In–As and In–P bonds with the Ga–P bond (54.9 kcal/mol) stronger than the Ga–As bond (50.1 kcal/mol), thus suppressing As/P exchange for GaAs-terminated surfaces. Regarding the growth technique, realization of wavelength-tunable InAs/InP QDs by metal-organic vapor-phase epitaxy (MOVPE) is highly desirable, which is the most common growth technique for optical devices operating in the 1.55-μm wavelength region and their monolithic integration on chip. Wavelength control of InAs/InP QDs, however, is anticipated to be most critical in

[a]Electronic mail: s.anantathanasarn@tue.nl

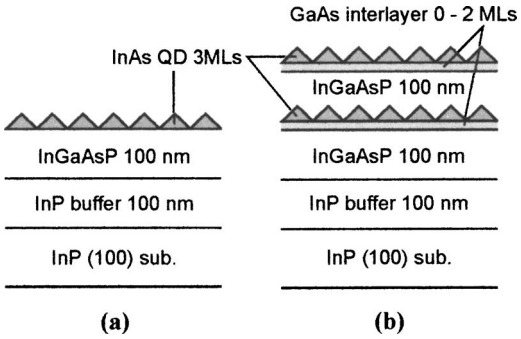

FIG. 1. (a) Sample structure A and (b) sample structure B.

MOVPE due to enhanced As/P exchange related to the higher growth temperature, high reactor pressure, long gas-phase diffusion, and complex gas switching and gas exchange processes. Up to now, only a few attempts to fabricate InP-based QD structures by MOVPE have been reported with typical emission wavelengths around 1.6 μm at RT.[10,11]

Here, we report the growth of InAs QDs embedded in an InGaAsP matrix, lattice-matched on InP (100) by MOVPE with tunable emission in the 1.55-μm wavelength region. The InGaAsP matrix with a band gap at λ_q=1.25 μm (Q1.25) is a standard waveguide core material in InP-based optoelectronic devices. Decrease of the QD growth temperature and V/III flow ratio reduces the QD size and emission wavelength due to suppression of As/P exchange. Precise control of the As/P exchange reaction and QD emission wavelength is then achieved by the insertion of an ultrathin GaAs interlayer underneath the QDs. An extended interruption after GaAs growth is essential to obtain well-defined InAs QDs. Submonolayer GaAs coverages result in a shape transition from QD to quantum dash at low V/III flow ratio, slightly shortening the emission wavelength. Only the combination of reduced growth temperature and V/III flow ratio with the insertion of GaAs interlayers above one-ML thickness allows wavelength tuning of the InAs QDs at room temperature in the 1.55-μm wavelength region. A GaAs interlayer thickness just above one ML produces the highest PL efficiency. Temperature-dependent PL measurements reveal zero-dimensional carrier confinement in the InAs QDs and confirm that the QDs are free of defects.

II. EXPERIMENT

The samples were grown by low-pressure MOVPE using trimethyl-indium (TMI), trimethyl-gallium (TMG), tertiarybutyl-arsine (TBA), and tertiarybutyl-phosphine (TBP) as gas sources with hydrogen as a carrier gas. The reactor pressure was 100 mbars and the total reactor flow was 15 000 SCCM (SCCM denotes cubic centimeter per minute at STP). The epiready InP (100) substrates, misoriented 2° toward (110), were thermally cleaned in the MOVPE reactor for 5 min at 600 °C (substrate temperatures refer to the thermocouple readout) under TBP flow before the substrate temperature was lowered for sample growth. Two sample structures were investigated, as shown in Figs. 1(a) and 1(b). Structure A consists of a 100-nm-thick InP buffer and a 100-nm-thick lattice-matched Q1.25 InGaAsP layer,

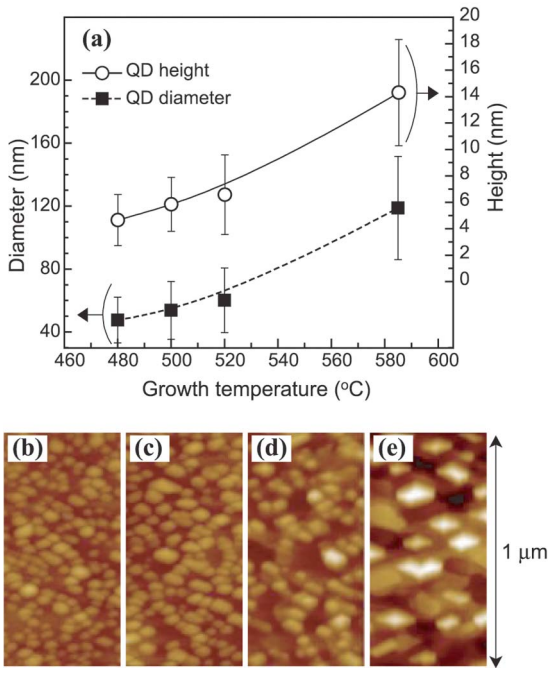

FIG. 2. (Color online) (a) QD height and base diameter as a function of growth temperature. (b)–(e) AFM images (0.5×1.0 μm^2) of the QDs of structure A grown at (b) 480, (c) 500, (d) 520, and (e) 585 °C. The height contrast is 40 nm in all images.

both grown at 585 °C, which was followed by the three-MLs InAs QD layer deposited at substrate temperatures between 480 and 585 °C and growth rates of 0.7–1.0 ML/s depending on temperature. In structure B, the whole layer sequence was grown at 500 °C with recalibrated gas-source flows for lattice-matched Q1.25 InGaAsP. The structure commenced with 100-nm InP and 100-nm InGaAsP followed by the GaAs interlayer with thickness of zero to two MLs (growth rate of 0.16 ML/s), the three-MLs InAs QDs grown with varied TBA flow, 5 s growth interruption in TBA, and the upper 100-nm InGaAsP layer. On top of this InGaAsP layer, growth of the GaAs interlayer and InAs QDs was repeated at the same conditions. The partial pressures of TMI and TBP of 0.0047 and 0.19 mbar were kept constant for all samples, while those of TMG and TBA were varied, as indicated in the respective sections. The morphology of the QDs on the sample surface was assessed by tapping-mode atomic force microscopy (AFM) in air. The inner crystalline structure of the samples was characterized by high-resolution x-ray diffraction (XRD). For the PL measurements a Nd:YAG (yttrium aluminum garnet) laser (532 nm) was used as an excitation source with excitation power density of 256 mW/cm^2. The samples were mounted in a He-flow cryostat for temperature control between 4.8 K and RT. The PL was dispersed by a single monochromator and recorded by a cooled (In,Ga) As charge-coupled device.

III. RESULTS AND DISCUSSION

A. Growth temperature

Figure 2(a) shows the height and base diameter of the InAs QDs grown at temperatures of 480, 500, 520, and 585 °C for structure A. The corresponding AFM images are

depicted in Figs. 2(b)–2(e). The TMG and TBA partial pressures are 0.0016 and 0.0070 mbar. The InAs QDs grown at our standard temperature of 585 °C exhibit heights of 10–20 nm and base diameters larger than 100 nm. These large QD dimensions are primarily attributed to strong As/P exchange at this high temperature. PL measurements of the QDs capped with InGaAsP at 585 °C reveal emission wavelengths, even at low temperature, longer than 1.6 μm, which is the detection limit of the cooled InGaAs detector. Attempts to shorten the emission wavelength by thin InP capping and annealing, annealing in TBA and/or TBP, or insertion of GaAs interlayers were not successful.

When the growth temperature is reduced, the InAs QD height and base diameter significantly decrease. The QD height, which dominates the carrier confinement, is, e.g., 5–6 nm for the QDs grown at 500 °C. Moreover the aspect ratio of the QDs (defined as height/base diameter) decreases from 0.14 to 0.09 for the QDs grown at 500 °C. This is consistent with the fact that at high temperatures, P atoms are easily desorbed from the surface due to the high P vapor pressure, leading to free In adatoms migrating toward the apex of the QDs similar to the case of InAs/InP.[4] Hence, the observed drastic change in QD dimensions confirms suppression of As/P exchange during growth at low temperature. This is in agreement with the reported exponential dependence of the As/P exchange reaction rate on the substrate temperature for InP surfaces.[3] In addition, the QD density is considerably increased at reduced growth temperature, being of the order of 10^{10} cm^{-2} at 500 °C, which is related to the shorter In adatom migration length.

B. GaAs interlayer at low growth temperature

As described above, a low growth temperature around 500 °C is essential for formation of small-and high-density QDs. When, however, the InAs QDs grown at low temperature are subsequently heated up to 585 °C under TBA flow for InGaAsP overgrowth, we observe an increase of the QD dimensions to values similar to those of the QDs directly grown at 585 °C due to thermally activated As/P exchange. Therefore, embedding small-and high-density QDs in InGaAsP requires a low growth temperature throughout the layer sequence. Here the use of TBP and TBA as gas sources for P and As is advantageous due to the lower pyrolysis temperatures, i.e., 450 and 425 °C for 50% pyrolysis of TBP and TBA compared to those of PH_3 and AsH_3 of 850 and 600 °C.[12] In fact, growth of InGaP by MOVPE at 520 °C using TMG and TBP as precursors has been demonstrated previously.[13] The gas source flows are recalibrated for growth of lattice-matched Q1.25 InGaAsP at 500 °C. In particular, the TMG flow is enhanced due to the reduced decomposition at low temperature, corresponding to the TMG partial pressure of 0.0016 mbar at 585 °C, which is increased to 0.0074 mbar at 500 °C. The TBA flow, however, is not changed much. The TBA partial pressure is 0.0070 mbar at 585 °C and 0.0059 mbar at 500 °C. Figure 3 shows a typical XRD spectrum in the vicinity of the symmetric (004) reflection of a sample of structure B grown at 500 °C with embedded three MLs InAs QD layer and two-MLs GaAs interlayer as example. The narrow zero-order peak and distinct diffraction fringes in the XRD spectrum confirm the high structural quality without prominent lattice defects or relaxation.

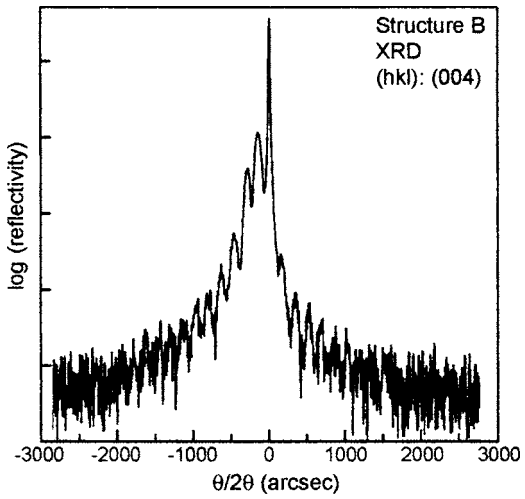

FIG. 3. XRD spectrum of a typical structure B recorded in the vicinity of the symmetric (004) reflection. The three-MLs InAs QDs embedded in an InGaAsP matrix with two-MLs GaAs interlayer are grown at 500 °C.

Figure 4(a) shows the PL spectra taken at 4.8 K of the InAs QDs of structure B without and with two-MLs GaAs interlayer and an additional flushing step under TBA flow. The corresponding QD morphologies on the sample surfaces are shown in Figs. 4(b)–4(d). The InAs QDs without a GaAs interlayer shown in Fig. 4(b) of structure B continuously grown at 500 °C are very similar to those of Fig. 2(c) also grown at 500 °C while the InGaAsP layer is grown at 585 °C, and they are similar to those grown by CBE with an average QD height of 6.0 nm. The PL peak emission wavelength, however, is beyond 1600 nm both at RT and 4.8 K, shown in Fig. 4(a). In order to shift the emission wavelength to shorter values, two-MLs GaAs is inserted on the InGaAsP layer underneath the InAs QDs. The two-MLs GaAs interlayer thickness is, from our previous experiments by CBE, the upper limit for defect-free structures, producing the largest possible blueshift of about 200 nm.[9] As shown in Fig. 4(c), the average QD height in the presence of the GaAs interlayer is reduced from 6.0 to 3.1 nm, and the peak emission wavelength reveals a blueshift to 1580 nm at 4.8 K, depicted in Fig. 4(a). As in CBE, the role of the GaAs interlayer is to effectively suppress the As/P exchange during InAs QD growth and to consume surface-segregated In on the InGaAsP layer, leading to a drastic reduction of the InAs QD height and, hence, PL emission wavelength.

The shoulder which is observed on the short-wavelength side of the PL spectrum of the InAs QDs with two-MLs GaAs interlayer [dash-dotted line in Fig. 4(a)] is attributed to composition inhomogeneities in the QD layer. These can easily arise due to the delayed gas exchange after switching in the MOVPE reactor causing a memory effect due to residual gas species. Therefore, we employ a flushing step of TMG under TBA flow after GaAs interlayer growth to ensure the presence of pure TMI as group-III source for QD growth. The flushing time in the present experiment is 45 s. The

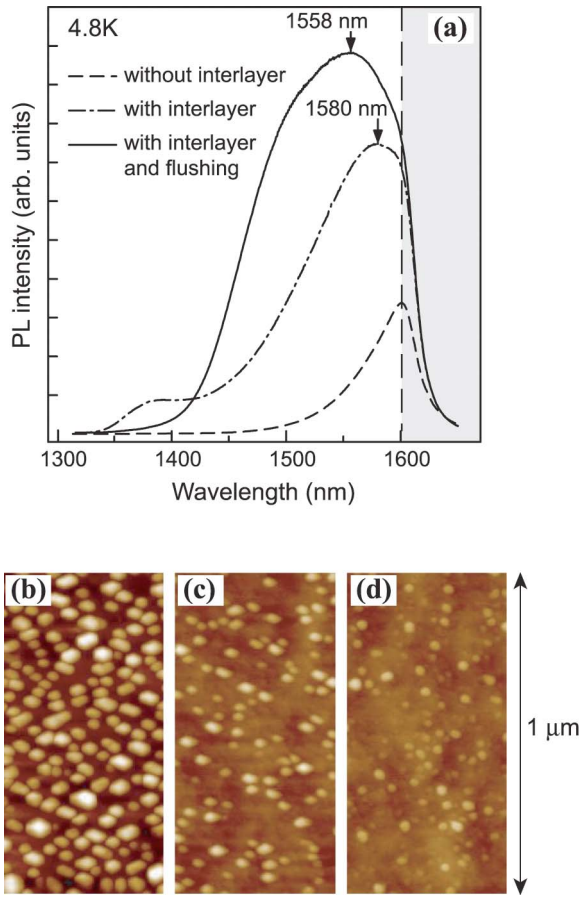

FIG. 4. (Color online) (a) PL spectra taken at 4.8 K of the three-MLs InAs QDs of structure B embedded in InGaAsP without GaAs interlayer (dashed line), with two-MLs GaAs interlayer (dash-dotted line), and with additional TMG flushing under TBA flow (solid line). The shaded area is above the detection limit of the cooled InGaAs detector at 1.6 μm. (b)–(d) AFM images (0.5×1.0 μm^2) of the corresponding QDs on the surface. The height contrast is 15 nm in all images.

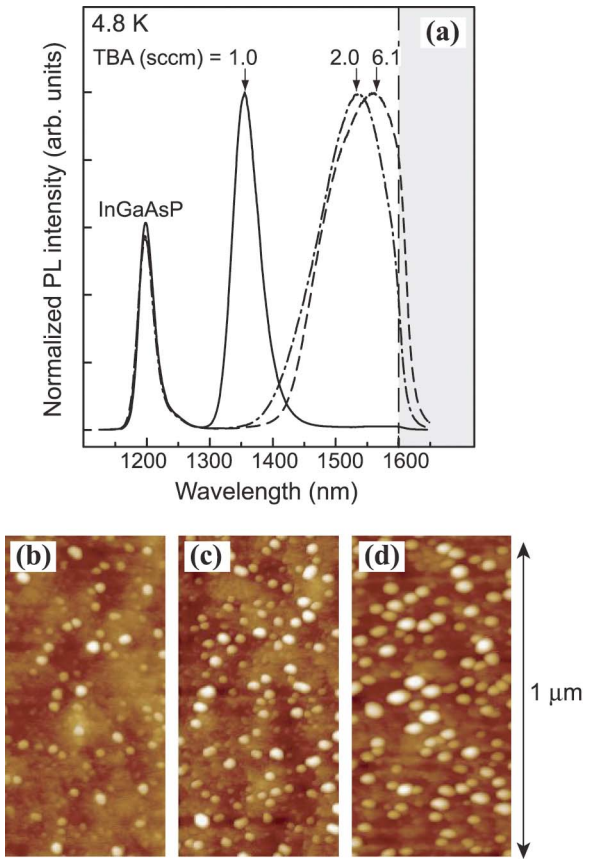

FIG. 5. (Color online) (a) Normalized PL spectra taken at 4.8 K of the three-MLs InAs QDs of structure B with two-MLs GaAs interlayer and additional TMG flushing under TBA flow. The TBA flow rate is varied between 6.1 and 1.0 SCCM while the TMI flow rate is kept constant. The shaded area is above the detection limit of the cooled InGaAs detector at 1.6 μm. (b)–(d) AFM images (0.5×1.0 μm^2) of the corresponding InAs QDs on the surface grown under the TBA flow rate of (b) 6.1, (c) 2.0, and (d) 1.0 SCCM. The height contrast is 10 nm in all images.

resulting InAs QDs are slightly smaller as shown in the AFM image of Fig. 4(d). This indicates increased lattice mismatch and, indeed, the presence of residual Ga in the InAs QD layer without flushing. The smaller QD size after flushing generates an additional blueshift of the PL peak emission wavelength to 1558 nm at 4.8 K, and no shoulder is observed in the PL spectrum, shown in Fig. 4(a).

C. V/III ratio

In order to study the effect of the V/III ratio on InAs QD formation, the TBA flow rate is reduced from 6.1 SCCM (TBA partial pressure of 0.0059 mbar) in the previous experiments to 2.0 SCCM (partial pressure of 0.0019 mbar) and 1.0 SCCM (partial pressure of 0.0009 mbar), while the TMI flow rate is kept constant. These TBA flow rates correspond to V/III ratios of 1.26, 0.4, and 0.2, calculated from the corresponding TBA and TMI partial pressures. The actual V/III ratios at the growing surface are, however, certainly larger since the pyrolysis of TMI is not 100% at the current growth temperature, while the pyrolysis of TBA is very efficient. This is deduced from the dependence of the incorporation efficiency of In and As on the growth temperature, which almost does not change for As but is reduced for In by a factor of 1.5 between 610 and 500 °C, as determined from XRD and PL measurements of InGaAsP layers. Also, some memory effect of TBA cannot be excluded to increase the actual V/III ratios, although the flushing for 45 s after GaAs interlayer growth under the reduced TBA flow is adopted to stabilize the low TBA partial pressure in addition to flushing out TMG.

The dependence of the PL spectra at 4.8 K on the TBA flow rate and the corresponding QD surface morphologies are shown in Fig. 5, again for InAs QDs grown on a two-MLs GaAs interlayer of structure B. For 6.1-SCCM TBA flow rate, the QD peak emission wavelength is 1558 nm at 4.8 K and beyond 1600 nm at RT despite of the small QD sizes. With reduction of the TBA flow, the PL of the QDs continuously shifts to shorter wavelengths, reaching a peak wavelength of 1355 nm at 4.8 K for the TBA flow rate of 1.0 SCCM. Simultaneously, the PL linewidth becomes smaller, pointing toward reduced As/P exchange under low TBA flow, reducing size fluctuations of the QDs in addition to shorten the emission wavelength. The increase of the QD diameter in Figs. 5(b)–5(d) likely arises from the interplay of increased As/P exchange reaction depth[14] at higher TBA flow and its suppression due to the GaAs interlayer being more efficient for lower TBA flow. The strong suppression of

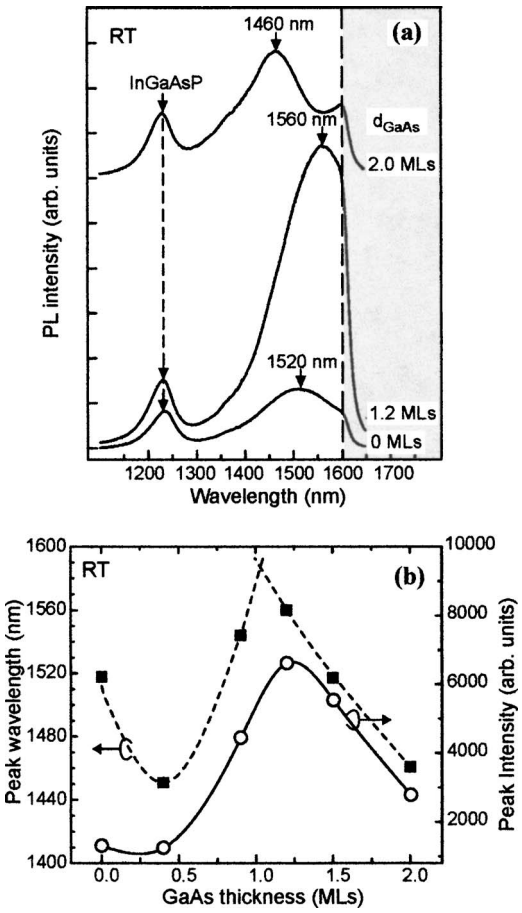

FIG. 6. (a) Room-temperature (RT) PL spectra of the three-MLs InAs QDs of structure B with GaAs interlayer thickness between zero and two MLs. The shaded area is above the detection limit of the cooled InGaAs detector at 1.6 μm. (b) Dependence of the PL peak wavelength and PL peak intensity of the InAs QDs on the GaAs interlayer thickness. The TBA flow rate is 1.0 SCCM.

As/P exchange, although the QDs become larger (wider) due to the larger In adatom migration length for low TBA flow, leads to QDs with shorter emission wavelength.

D. Wavelength tuning by GaAs interlayer thickness

After establishing the growth conditions such as substrate temperature, gas switching sequences, and group V/III ratio for obtaining a QD peak emission wavelength around 1450 nm at RT in the presence of a two-MLs GaAs interlayer (constituting the upper thickness limit for defect-free QDs), the emission wavelength of the QDs is tuned over the 1.55-μm wavelength region by reducing the GaAs interlayer thickness, anticipating the 200-nm wavelength shift obtained in CBE. The TBA flow rate is kept at 1.0 SCCM, the growth temperature is at 500 °C, and the flushing time after GaAs interlayer growth is at 45 s under the 1.0-SCCM TBA flow rate. Figure 6(a) shows the PL spectra taken at RT of the QDs of structure B for GaAs interlayer thicknesses of 2.0, 1.2, and 0 MLs. The QD peak emission wavelengths and the PL peak intensities as a function of GaAs interlayer thickness are summarized in Fig. 6(b).

When the GaAs interlayer thickness is reduced from 2.0 to 1.2 MLs, the PL peak emission wavelength continuously

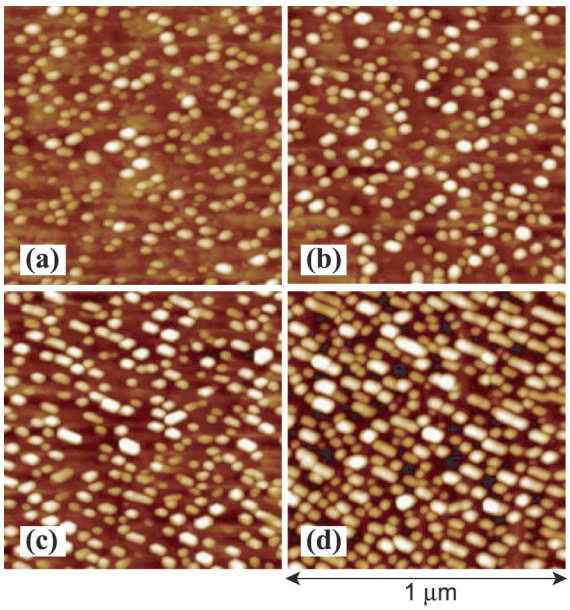

FIG. 7. (Color online) AFM images (1.0×1.0 μm^2) of the three-MLs InAs QDs on the surface of structure B with GaAs interlayer thickness of (a) 2.0, (b) 1.2, (c) 0.4, and (d) 0 MLs. The TBA flow rate is 1.0 SCCM. The height contrast is 10 nm in all images.

shifts to larger values from 1460 nm for two-MLs GaAs to 1560 nm for 1.2-MLs GaAs, covering the 1.55-μm wavelength region. Simultaneously, the PL efficiency improves, which is attributed to the reduction of tensile strain for thinner GaAs interlayers, improving the structural quality of the QDs. The morphology of the InAs QDs as a function of GaAs interlayer thickness is shown in Fig. 7. The average QD height increases from 4.5 nm for two-MLs GaAs [Fig. 7(a)] to 5.6 nm for the GaAs interlayer thickness of 1.2 MLs [Fig. 7(b)]. This confirms the continuous reduction of As/P exchange and consumption of surface-segregated In with GaAs interlayer thickness to continuously reduce the QD height and, hence, the peak emission wavelength.

Surprisingly, the PL peak emission wavelength in Fig. 6(b) shortens when the GaAs interlayer thickness is reduced to below one ML. This observation is understood by the surface morphology shown in Figs. 7(c) and 7(d). For GaAs interlayer thicknesses below one ML, a gradual morphological shape transition from QDs to quantum dashes elongated along [0-11] takes place. Quantum-dash formation was observed previously in the case of InAs/InP grown by MBE[15] and for the growth of InAs on InGaAs/InP (100).[16] Obviously the low group-V flow changes the properties of the InGaAsP surface to cause anisotropic surface diffusion along [0-11] leading to quantum-dash formation for submonolayer GaAs coverages. The low TBA flow, moreover, favors P incorporation into the quantum dashes during InAs growth causing the blueshift of the PL emission, which cannot be simply related to geometrical features. A detailed investigation of the shape transition and quantum-dash formation is, however, beyond the scope of the present investigation. The PL peak emission wavelength is shortest for 0.4-MLs GaAs and increases slightly without GaAs interlayer [Fig. 6(b)]. This is attributed to the interplay between shape transition, shortening the PL peak emission wavelength, and As/P ex-

change, increasing the quantum-dash height and PL peak emission wavelength with reduction of the GaAs interlayer thickness in the submonolayer range. Correlated with the shape transition from QDs to quantum dashes is a reduction of the PL peak intensity which is attributed to the larger lateral size of the quantum dashes, easily introducing defects.

It is important to note that only the combination of low growth temperature and V/III ratio with the insertion of GaAs interlayers allows continuous tuning of the QD emission wavelength over the 1.55-μm region. The low V/III ratio required to shift the QD emission wavelength, even in the presence of a GaAs interlayer, close to or slightly below 1.55 μm inevitably results in the formation of quantum dashes on InGaAsP. Moreover, the relationship between V/III ratio and GaAs interlayer thickness is optimized when the target peak emission wavelength of the QDs between 1.55 and 1.56 μm is reached for a GaAs interlayer thickness just above one ML, providing the highest possible QD PL peak intensity. This is most easily adjusted when reducing the V/III ratio in the presence of the thickest possible GaAs interlayer (two MLs) to shift the PL peak emission wavelength to the short-wavelength limit of the tuning range, which is at around 1450 nm at RT for a full tuning range of about 200 nm as a function of GaAs interlayer thickness between zero and two MLs. This is demonstrated in our experiments. The continuous wavelength tuning of the InAs QDs with the GaAs interlayer thickness is most convenient to compensate for additional wavelength redshifts in stacked QD layers[17] for applications in photonic devices operating in the 1.55-μm wavelength region. Experiments with GaP interlayers, shifting the QD peak emission wavelength to 1.55 μm in CBE for submonolayer coverages,[18] were not successful. The RT PL efficiency was very weak, most probably due to a higher sensitivity of MOVPE growth to the high tensile strain of GaP introducing defects in the QDs.

E. Optical properties of QDs emitting at 1.55 μm

Detailed temperature-dependent PL measurements between 4.8 K and RT of the QDs with 1.2-MLs GaAs interlayer emitting at 1560 nm at RT reveal zero-dimensional carrier confinement and excellent optical quality of the QDs. Figure 8(a) shows the QD PL peak energy and linewidth as a function of temperature. The behavior of both the PL peak energy and linewidth is similar to that of InAs/GaAs QDs[19,20] and of the CBE-grown InAs/InGaAsP/InP QDs,[18] originating from the zero-dimensional confinement of carriers in inhomogeneous QD ensembles. The PL linewidth undergoes a minimum around 100 K due to thermally activated carrier redistribution, preferentially from smaller (higher energy) to larger (lower energy) QDs which is followed by equilibration of the carrier distribution at higher temperatures when thermally activated carrier escape from smaller and larger QDs becomes comparable. In the same temperature range between 50 and 170 K the PL peak energy reveals a low-energy shift, which is much steeper than that of the band gap according to the empirical Varshni law for InAs [dashed line in Fig. 8(a)], reflecting the preferential carrier occupation of larger QDs.

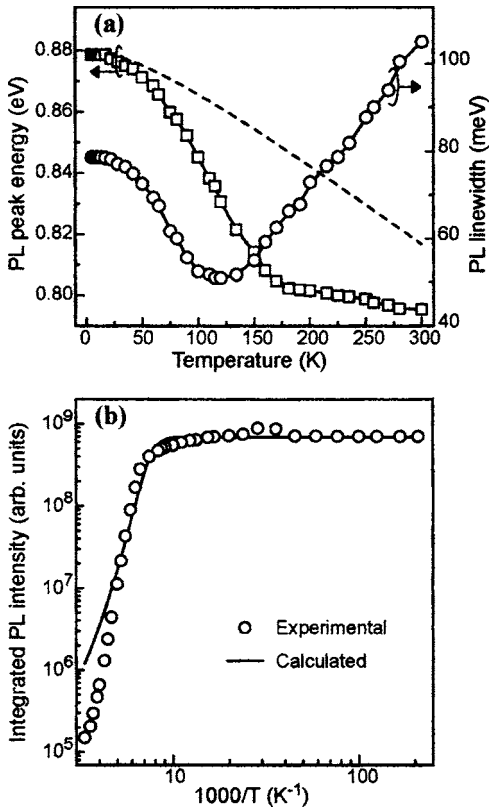

FIG. 8. (a) Temperature dependence of the PL peak energy and PL linewidth of the three-MLs InAs QDs with 1.2-MLs GaAs interlayer. The dashed line is the temperature dependence of the InAs band-gap energy according to the Varshni law, assuming E_g=0.88 eV at T=0 K. (b) Integrated PL intensity of the InAs QDs as a function of temperature. The solid line is the exponential fit with a thermal activation energy of 145 meV.

The integrated PL intensity of the InAs QDs shown in Fig. 8(b) is almost constant up to 140 K and decreases exponentially at higher temperatures. The activation energy (E_a) describing the quenching of the PL intensity is derived from a fit to the following expression:

$$I_{\mathrm{PL}} = \frac{C}{1 + Ae^{-E_a/k_B T}}, \tag{1}$$

where k_B is the Boltzmann constant and T is the temperature. C and A are fitting parameters. The activation energy amounts to 145 meV, which is close to the difference of the InGaAsP band-gap energy and the InAs QD emission energy of 152 meV. Hence, the almost constant integrated PL intensity up to 140 K where substantial carrier redistribution takes place and the subsequent PL intensity quenching which is consistent with thermionic emission of carriers from the InAs QDs into the InGaAsP barriers confirm the excellent optical quality of the QDs, which are free of nonradiative recombination centers.

IV. CONCLUSION

In summary, we have reported the growth of wavelength-tunable InAs QDs embedded in a lattice-matched InGaAsP matrix on InP (100) by MOVPE. As/P exchange, shifting the emission wavelength of the QDs beyond 1.6 μm at room temperature (RT), has been suppressed

by decreasing the QD growth temperature and the V/III flow ratio. The QD emission wavelength was then reproducibly tuned over the 1.55-μm wavelength region by the thickness of an ultrathin (zero to two MLs) GaAs interlayer underneath the QDs, controlling the As/P exchange reaction. An extended interruption after GaAs interlayer growth was essential to obtain well-defined InAs QDs. Submonolayer GaAs coverages resulted in a shape transition from QD to quantum dash at low V/III flow ratio with a slightly shorter emission wavelength. Only the combination of reduced growth temperature and V/III flow ratio with the insertion of GaAs interlayers above one-ML thickness allowed wavelength tuning of QDs at RT in the technologically important 1.55-μm wavelength region for fiber-optical telecommunication systems. A GaAs interlayer thickness just above one ML produced the highest PL efficiency. Temperature-dependent PL measurements revealed zero-dimensional carrier confinement in the defect-free InAs QDs.

ACKNOWLEDGMENT

Part of the work was supported by the IS project "Optoelectronic large scale integration," project No. IS-041045, Senter Novem, The Netherlands.

[1]Y. Arakawa and H. Sakaki, Appl. Phys. Lett. **40**, 939 (1982).
[2]M. Asada, Y. Miyamoto, and Y. Suematsu, IEEE J. Quantum Electron. **QE-22**, 1915 (1986).
[3]Y. Kobayashi and N. Kobayashi, Jpn. J. Appl. Phys., Part 1 **31**, 3988 (1992).
[4]S. Yoon, Y. Moon, T.-W. Lee, E. Yoon, and Y. D. Kim, Appl. Phys. Lett. **74**, 2029 (1999).
[5]M. Borgström, J. Johansson, L. Landin, and W. Seifert, Appl. Surf. Sci. **165**, 241 (2000).
[6]B. Wang, F. Zhao, Y. Peng, Z. Jin, Y. Li, and S. Liu, Appl. Phys. Lett. **72**, 2433 (1998).
[7]Y. Sakuma, K. Taketomo, S. Hirose, T. Usuki, and N. Yokoyama, Physica E (Amsterdam) **26**, 81 (2005).
[8]R. Schwertberger, D. Gold, J. P. Reithmaier, and A. Forchel, J. Cryst. Growth **251**, 248 (2003).
[9]Q. Gong, R. Nötzel, P. J. van Veldhoven, T. J. Eijkemans, and J. H. Wolter, Appl. Phys. Lett. **84**, 275 (2004).
[10]K. Kawaguchi, M. Ekawa, A. Kuramata, T. Akiyama, H. Ebe, M. Sugawara, and Y. Arakawa, Appl. Phys. Lett. **85**, 4331 (2004).
[11]W. G. Jeong, P. D. Dapkus, U. H. Lee, J. S. Yim, D. Lee, and B. T. Lee, Appl. Phys. Lett. **78**, 1171 (2001).
[12]G. B. Stringfellow, *Organometallic Vapor-Phase Epitaxy: Theory and Practice*, 2nd ed. (Academic, New York, 1999).
[13]H. Murata, I. H. Ho, and G. B. Stringfellow, J. Cryst. Growth **170**, 219 (1997).
[14]K. Y. Suh, H. H. Lee, and E. Yoon, J. Appl. Phys. **85**, 233 (1999).
[15]M. Gendry *et al.*, J. Appl. Phys. **95**, 4761 (2004).
[16]A. Stintz, T. J. Rotter, and K. J. Malloy, J. Cryst. Growth **255**, 266 (2003).
[17]M. P. Pires, S. M. Landi, C. V.-B. Tribuzy, L. A. Nunes, E. Marega, and P. L. Souza, J. Cryst. Growth **272**, 192 (2004).
[18]Q. Gong, R. Nötzel, P. J. van Veldhoven, T. J. Eijkemans, and J. H. Wolter, Appl. Phys. Lett. **85**, 1404 (2004).
[19]Z. Y. Xu *et al.*, Phys. Rev. B **54**, 11528 (1996).
[20]D. I. Lubyshev, P. P. González-Borrero, E. Marega, Jr., E. Petitprez, N. La Scala, Jr., and P. Basmaji, Appl. Phys. Lett. **68**, 205 (1996).